



This paper is a part of the hereunder thematic dossier published in OGST Journal, Vol. 68, No. 5, pp. 789-946 and available online [here](#)

Cet article fait partie du dossier thématique ci-dessous publié dans la revue OGST, Vol. 68, n°5, pp. 789-946 et téléchargeable [ici](#)

DOSSIER Edited by/Sous la direction de : **A. Daudin et A. Quignard**

## PART 2

### Second and Third Generation Biofuels: Towards Sustainability and Competitiveness

#### Deuxième et troisième génération de biocarburants : développement durable et compétitivité

*Oil & Gas Science and Technology – Rev. IFP Energies nouvelles*, Vol. 68 (2013), No. 5, pp. 789-946

Copyright © 2013, IFP Energies nouvelles

- 789 > Editorial
- 801 > *Biomass Fast Pyrolysis Reactors: A Review of a Few Scientific Challenges and of Related Recommended Research Topics*  
Réacteur de pyrolyse rapide de la biomasse : une revue de quelques verrous scientifiques et d'actions de recherches recommandées  
J. Lédé
- 815 > *Membrane Fractionation of Biomass Fast Pyrolysis Oil and Impact of its Presence on a Petroleum Gas Oil Hydrotreatment*  
Fractionnement membranaire d'une huile de pyrolyse flash et impact de sa présence sur l'hydrotraitement d'un gazole atmosphérique  
A. Pinheiro, D. Hudebine, N. Dupassieux, N. Charon and C. Geantet
- 829 > *Hydrodeoxygenation of Phenolic Compounds by Sulfided (Co)Mo/Al<sub>2</sub>O<sub>3</sub> Catalysts, a Combined Experimental and Theoretical Study*  
Hydrodésoxygénation de composés phénoliques en présence de catalyseurs sulfurés (Co)Mo/Al<sub>2</sub>O<sub>3</sub> : une étude expérimentale et théorique  
M. Badawi, J.-F. Paul, E. Payen, Y. Romero, F. Richard, S. Brunet, A. Popov, E. Kondratieva, J.-P. Gilson, L. Mariey, A. Travert and F. Maugé
- 841 > *Transformation of Sorbitol to Biofuels by Heterogeneous Catalysis: Chemical and Industrial Considerations*  
Transformation du sorbitol en biocarburants par catalyse hétérogène : considérations chimiques et industrielles  
L. Vilcocq, A. Cabiac, C. Espezel, E. Guillon and D. Duprez
- 861 > *Biomass Conversion to Hydrocarbon Fuels Using the MixAlco™ Process*  
Conversion de la biomasse en combustibles hydrocarbonés au moyen du procédé MixAlco™  
S. Taco-Vasquez and M.T. Holtzapple
- 875 > *Algogroup: Towards a Shared Vision of the Possible Deployment of Algae to Biofuels*  
Algogroup : vers une vision partagée du possible déploiement de la conversion des algues en carburants  
X. Montagne, P. Porot, C. Aymard, C. Querleu, A. Bouter, D. Lorne, J.-P. Cadoret, I. Lombaert-Valot and O. Petillon
- 899 > *Towards a Microbial Production of Fatty Acids as Precursors of Biokerosene from Glucose and Xylose*  
Vers une production microbienne d'acides gras en vue de l'application biokérosène à partir de glucose et xylose  
M. Babau, J. Cescut, Y. Allouche, I. Lombaert-Valot, L. Fillaudeau, J.-L. Uribelarrea and C. Molina-Jouve
- 913 > *Insight on Biomass Supply and Feedstock Definition for Fischer-Tropsch Based BTL Processes*  
Aperçu sur l'approvisionnement en biomasse et la caractérisation des charges pour les procédés de synthèse de biocarburants par voie BTL  
J. Coignac
- 925 > *Second Generation Gaseous Biofuels: from Biomass to Gas Grid*  
Biocarburants gazeux de 2<sup>e</sup> génération : du gisement de biomasse au réseau de gaz  
O. Guerrini, M. Perrin and B. Marchand
- 935 > *BioTfuel Project: Targeting the Development of Second-Generation Biodiesel and Biojet Fuels*  
Le projet BioTfuel : un projet de développement de biogazole et biokérosène de 2<sup>e</sup> génération  
J.-C. Vigié, N. Ullrich, P. Porot, L. Bournay, M. Hecquet and J. Rousseau

# Biomass Conversion to Hydrocarbon Fuels Using the MixAlco™ Process

S. Taco-Vasquez\* and M.T. Holtzapple

Department of Chemical Engineering, Texas A&M University, College Station, TX 77843-3122 - United States  
e-mail: sebrisco@hotmail.com - m-holtzapple@mail.che.tamu.edu

\* Corresponding author

**Résumé — Conversion de la biomasse en combustibles hydrocarbonés au moyen du procédé MixAlco™** — Le procédé MixAlco™ convertit la biomasse en hydrocarbures (par exemple, en essence) selon les étapes génériques suivantes : prétraitement, fermentation, écumage, déshydratation, cétonisation thermique, distillation, hydrogénation, oligomérisation et saturation. Cette étude décrit la production de bioessence à partir de fumier de poulet et de papier en lambeaux, ces deux sources étant des matières premières convoitées ne nécessitant pas de prétraitement. À l'aide d'une culture mixte de microorganismes dérivés de sols marins, la biomasse a été soumise à une fermentation de manière à produire une solution aqueuse diluée de sels de carboxylates, ultérieurement écumés et séchés. Les sels séchés ont été thermiquement convertis en cétones brutes, ensuite distillées afin d'éliminer les impuretés. À l'aide du catalyseur à base de nickel de Raney, les cétones distillées ont été hydrogénées en alcools secondaires mixtes allant de C3 à C12. En utilisant le catalyseur supporté sur zéolite HZSM-5, ces alcools ont été oligomérisés en hydrocarbures dans un réacteur à écoulement piston. Enfin, ces hydrocarbures insaturés ont été hydrogénés afin de produire un mélange d'hydrocarbures pouvant être combiné à l'essence commerciale.

**Abstract — Biomass Conversion to Hydrocarbon Fuels Using the MixAlco™ Process** — The MixAlco™ process converts biomass to hydrocarbons (e.g., gasoline) using the following generic steps: pretreatment, fermentation, descumming, dewatering, thermal ketonization, distillation, hydrogenation, oligomerization and saturation. This study describes the production of bio-gasoline from chicken manure and shredded office paper, both desirable feedstocks that do not require pretreatment. Using a mixed culture of microorganisms derived from marine soil, the biomass was fermented to produce a dilute aqueous solution of carboxylate salts, which were subsequently descummed and dried. The dry salts were thermally converted to raw ketones, which were distilled to remove impurities. Using Raney nickel catalyst, the distilled ketones were hydrogenated to mixed secondary alcohols ranging from C3 to C12. Using zeolite HZSM-5 catalyst, these alcohols were oligomerized to hydrocarbons in a plug-flow reactor. Finally, these unsaturated hydrocarbons were hydrogenated to produce a mixture of hydrocarbons that can be blended into commercial gasoline.

## INTRODUCTION

High global demand for liquid transportation fuels and the depletion of conventional crude oil have motivated research into alternative fuels. Many options exist, such as the production of liquid hydrocarbons from tar sands, shale, coal or natural gas. All of these options are based on fossil fuels, which are a finite resource. Further, the combustion of fossil fuels accumulates carbon dioxide into the atmosphere, which is implicated in global warming.

The production of liquid transportation fuels from biomass is an attractive alternative – biomass is renewable and its combustion does not contribute net carbon dioxide to the environment. Currently, at a commercial scale, sugarcane (Brazil) and corn (United States) are converted to ethanol. As a stop-gap measure, this is acceptable; however, it is not a viable long-term solution. Both these approaches use food as a feedstock, which raises food prices. Per-hectare yields of fuel are relatively low, thus requiring excessive land area to meet the large demand for liquid transportation fuels. Ethanol is a less-than-ideal fuel because it has a low energy content compared to hydrocarbons. Because it is hydroscopic, it cannot be shipped through common-carrier pipelines and thus requires special handling. Common engines are not able to combust fuel that contains more than about 10% ethanol, so there is a limit to the amount that can be incorporated into the fuel supply without major overhaul of the transportation infrastructure.

Rather than using food as feedstock for producing biofuels, lignocellulose is a superior alternative. Examples of lignocellulose are wood and grasses, which typically contain cellulose (38-50%), hemicellulose (23-32%) and lignin (15-30%). Some lignocellulose feedstocks (*e.g.*, poplar, energy cane, miscanthus, sorghum) have very high per-hectare yields. Also, lignocellulose is a common component of waste streams, such as municipal solid waste, sewage sludge, manure and agriculture residues.

Ideally, rather than converting lignocellulose to ethanol, it would be converted to hydrocarbons that are similar to those currently produced from fossil fuels, which would be completely compatible with our current infrastructure. One option is the MixAlco™ process, which converts lignocellulose into hydrocarbon fuels (*e.g.*, gasoline). Preliminary economic studies indicate that bio-gasoline can be sold for \$2.56/gal (\$0.68/L) in a base-case scenario [1]. The selling price can range from \$1.25/gal (\$0.33/L) to \$3.75/gal (\$0.99/L), depending upon assumptions.

The MixAlco™ process is a version of the carboxylate platform that does not require sterilization to obtain fuels [1-4]. Using a fermentation process similar to that which occurs in the rumen of cattle, the biomass is converted to mixed acids (*e.g.*, acetic, propionic, butyric acid). Using a buffer (*e.g.*, calcium carbonate), these acids are neutralized to their corresponding carboxylate salts, which are subsequently chemically transformed into a variety of industrial chemicals (*e.g.*, acetone, isopropanol) or fuels (*e.g.*, gasoline, jet fuel).

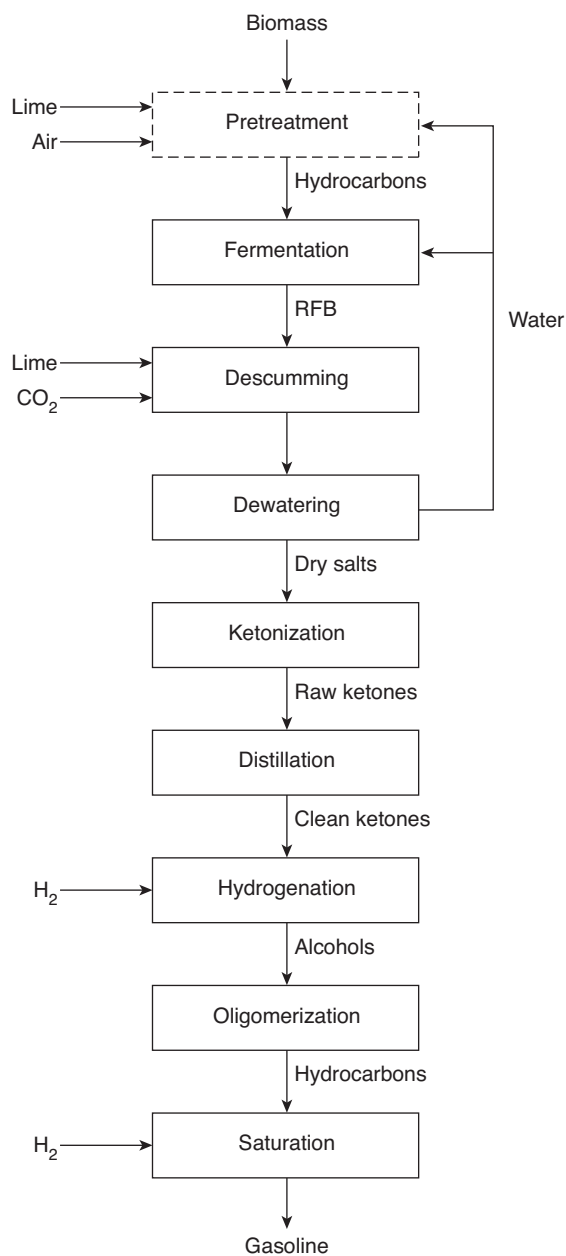


Figure 1

Simplified process block diagram of the MixAlco™ process. (Note: the process presented in this study excluded the pretreatment step).

Figure 1 illustrates each step in the MixAlco™ process. If the biomass source has a high lignin content (*e.g.*, agricultural residues, energy crops, wood), the lignocellulose is pretreated with lime and air, which enhances digestibility by removing lignin. Alternatively, if the biomass source has a low lignin content (*e.g.*, waste paper, food scraps), the pretreatment step can be eliminated. Then, using a mixed

culture of microorganisms derived from marine soil, the pretreated lignocellulose is fermented to Raw Fermentation Broth (RFB), an aqueous mixture of carboxylate salts (C2–C7), nutrients, microorganisms and impurities. In the descumming step, RFB is treated with lime followed by CO<sub>2</sub>, which precipitates calcium carbonate and eliminates many of the impurities. The descummed RFB is dewatered by evaporation, which crystallizes the carboxylate salts. In a batch reactor [5], the salts are thermochemically transformed into raw ketones, which are distilled and then hydrogenated to mixed alcohols [6]. In a Plug-Flow Reactor (PFR), the mixed alcohols are dehydrated and oligomerized using a zeolite catalyst. Finally, the unsaturated hydrocarbons are hydrogenated in a batch reactor to obtain gasoline.

This paper presents results from pilot-scale production of hydrocarbons using the MixAlco™ process. The emphasis was to produce intermediates typical of what would be produced in an industrial process. Finally, these intermediates were converted to bio-gasoline.

## 1 DETAILED PROCESS DESCRIPTION

As described in Figure 1, biomass is processed through a variety of steps resulting in intermediates (ketones, alcohols) that can be used as industrial chemicals. In principal, these intermediates also could be used as fuels; however, they are not compatible with our current infrastructure, so they are converted to liquid hydrocarbons (*e.g.*, gasoline).

The biomass fed to the fermentor must contain a source of energy (*e.g.*, municipal solid waste, corn stover, office paper, paper fines, rice straw and water hyacinths) and a source of nutrients (food scraps, sewage sludge or manure). In addition, chemical nutrients (*e.g.*, urea, ammonia, ammonium bicarbonate) can be added to supply essential minerals.

### 1.1 Pretreatment

In nature, lignocellulose is used as a structural component (*e.g.*, stems, branches, leaves), so it is designed to resist biodegradation. To overcome this natural resistance, pretreatment is necessary. Factors that affect the digestibility include the following: lignin content, acetyl content of hemicellulose, cellulose crystallinity, degree of cellulose polymerization, biomass particle size, pore volume and accessible surface area [7]. Chang and Holtzapple [8] studied how lignin, acetyl groups and crystallinity affect the digestibility. They created 147 biomass samples with varying lignin contents, acetyl groups and crystallinities and concluded that acetyl groups have the least impact on biomass digestibility. However, it is easy to remove them with alkali, so there is little cost. The acetyl groups contribute a minor amount to the final acid concentration in the fermentation. Lignin removal primarily affects the ultimate biomass conversion. Cellulose crystallinity

increases hydrolysis rates and improves ultimate conversion. (Note: in this study, pretreatment was not performed because the biomass source had low lignin content and was very digestible).

Figure 2 depicts a schematic of a pretreatment that uses lime, water and air to remove lignin and acetyl groups from biomass. The biomass is piled on top of a gravel bed lined with geomembrane. A perforated PVC pipe is embedded in the gravel, which allows air to flow upward through the bed. Water is pumped from the gravel to the top of the pile to ensure that it stays wetted. Typical operating conditions are  $T = 55^{\circ}\text{C}$ ,  $t = 2$  to 4 weeks and lime loading = 0.1 to 0.15 g Ca(OH)<sub>2</sub>/g dry biomass.

### 1.2 Fermentation

In this study, shredded office paper (98%) and chicken manure (2%) were the biomass feedstocks. Because lignin was removed in the paper pulping process, further pretreatment of the shredded office paper was not necessary. Table 1 shows typical feedstock properties used for the fermentation.

Four 3780-L fermentors operated in parallel. Figure 3 shows the schematic flow diagram of each fermentor. The fermentors were started in batch mode; thereafter, they operated in fed-batch mode. In the fed-batch mode, every 7-10 days, about 80 to 100 kg of dry shredded paper, dechlorinated water (1 700-1 900 L) and 1.5-2 kg (dry basis) chicken manure were added manually to the top of each fermentor (*Fig. 4*). About 80 to 85% of fermentor volume was used. From the top, the fermentor was mixed manually using a paddle. To facilitate microbial metabolic activity, fertilizer-grade urea was added to the fermentor to maintain a C/N ratio of 30 g C/g N. The fermentation reaction was performed anaerobically at 40°C by circulating warm water through coiled tubing surrounding the fermentor. The pH ranged from 5.5-7.0. The fermentor was operated using non-sterile conditions. The inoculum was marine soil from Galveston, Texas, USA. No buffer was required; the minerals naturally present in the feedstock provided sufficient buffering.

TABLE 1  
Characteristics of fermentation feedstocks

Properties	Shredded waste office paper	Fresh chicken manure	Urea
Moisture content, $M$ (g/100 g of wet sample)	3.75 ± 0.75	80.67 ± 3.45	0.0
Ash content, $I$ (g/100 g of dry sample)	16.92 ± 0.70	47.55 ± 1.25	0.0
Carbon content, $C$ (g/100 g dry sample)	40.35 ± 1.56	28.82 ± 3.58	19.97 ± 0.72
Nitrogen content, $N$ (g/100 g dry sample)	0.13 ± 0.05	1.81 ± 0.36	45.26 ± 0.50

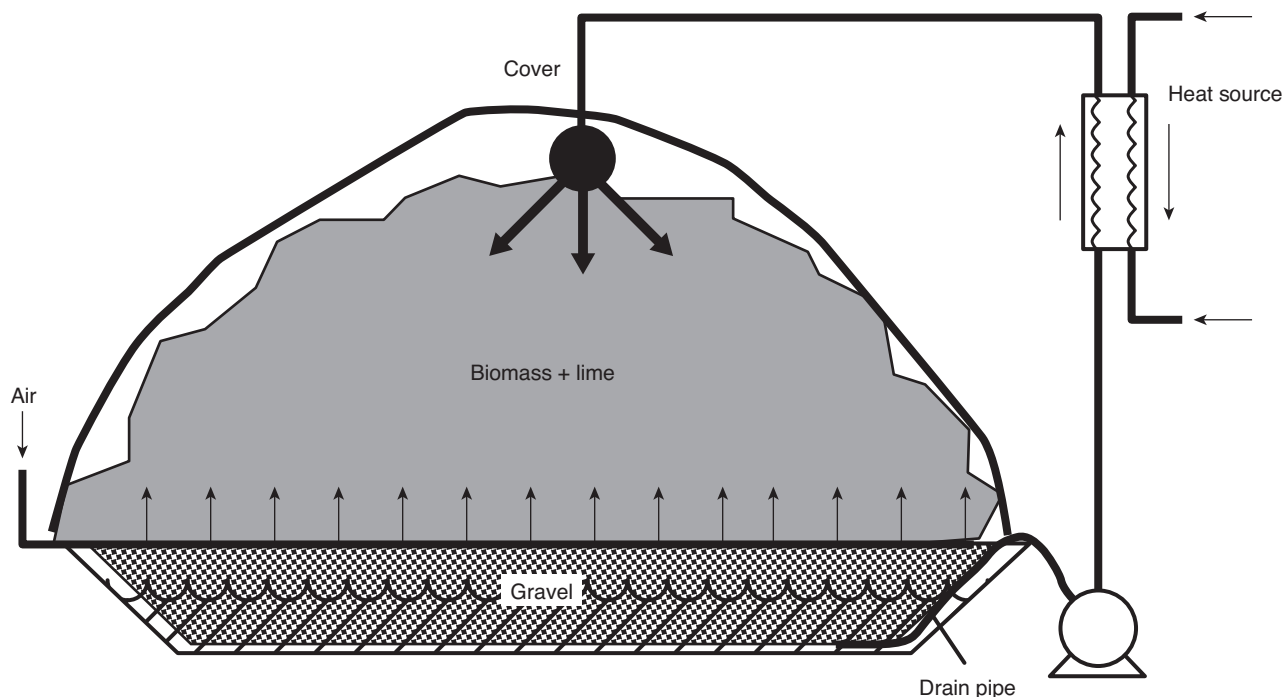


Figure 2

Biomass pretreatment with lime and air. (Note: the process used in this study excluded the pretreatment step).

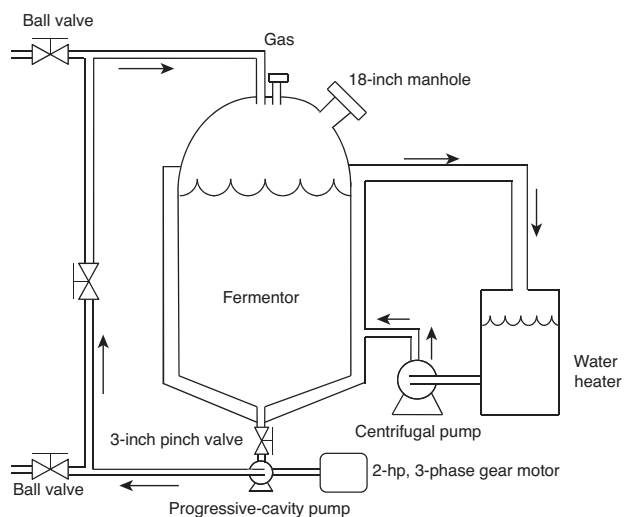


Figure 3

Schematic process flow diagram of the fermentor.



Figure 4

Top section of the four pilot-plant fermentors including the cat-walk.

To suppress methanogens, iodoform (20 g/L ethanol) was added to each fermentor (200-800 mL per day). This iodoform solution was mixed into the fermentation broth using a progressive-cavity sludge pump (*Moyno 1000 series, Model B1E-CDQ-AAA, Fig. 3*), which ran almost every day for 1 h.

When the fermentors were operated in fed-batch mode, every 7-10 days, broth was harvested from the top of the fermentor using a submersible pump. All the liquid was removed, leaving the water-saturated undigested paper sludge in the fermentor. Then, the undigested paper sludge

was collected by opening the ball valve (*Fig. 3*) and pumping using the progressive-cavity pump. Before disposing the undigested solids, the liquid was extracted from the solids using a screw press (Vincent Compact Screw Press; Model: CP-6; Vincent Corporation, Florida, USA), which allowed recovery of carboxylate salts from the liquid. Then, the solids were washed with water and pressed again to remove the remaining salts. This washed water was recycled to the fermentor with fresh water required for the next fermentation.

After harvesting the fermentation broth, about  $760 \pm 190$  L of wet semi-digested fermentation sludge from the previous batch was left in the fermentor as inocula.

### 1.3 Descumming

Raw Fermentation Broth (RFB) – the liquid obtained from the fermentation process – contained organic scum, which included suspended paper particles, microorganisms and proteins. To purify RFB, >95% of the scum had to be removed to improve salt quality and avoid fouling in the dewatering process. Descumming was a batch process. A positive-displacement pump loaded 1 890 L of RFB into a 2 270-L stainless steel steam-jacketed mixing tank. The tank was heated to about 80-90°C. Then, industrial-grade slaked lime ( $\text{Ca}(\text{OH})_2$ ) was added to increase the broth pH from 5.5-7 to 10.5-11.5. During lime addition, the tank was continuously mixed by circulating the broth using a high-temperature centrifugal pump. Thereafter,  $\text{CO}_2$  gas was bubbled from a liquid  $\text{CO}_2$  cylinder to remove excess  $\text{Ca}(\text{OH})_2$  as  $\text{CaCO}_3$ .

The formation of  $\text{CaCO}_3$  particles helped to nucleate and agglomerate scum. When the flocculation was complete, the descummed broth was transferred to a tank for cooling and storage. Then, the 2 270-L mixing tank was cleaned for the next cycle.

To remove the precipitated scum, the broth was centrifuged (1 700 rpm, 7 gpm, Model # MAPX-204 centrifuge, Alfa Laval Inc.). By precipitating  $\text{CaCO}_3$  from the mother liquor, it was possible to recover more than 95% of salts from the broth. After centrifuging, the clarified liquid broth passed to the dewatering step.

### 1.4 Dewatering

The 2 270-L stainless steel steam-jacketed tank was used for both descumming and dewatering. In each batch, about 1 890 L of descummed-and-centrifuged broth was fed to the 2 270-L tank and boiled with steam generated from a propane-heated boiler (Model # 103, Parker Boiler Co.). When half the liquid broth evaporated, the salts started precipitating. The concentrated broth from the 2 270-L tank was transferred to a 1 130-L steam-jacketed tank for further concentration and crystallization.

First, the high-molecular-weight calcium salts precipitated and floated to the top. A fine-mesh stainless steel screen was

used to skim the floating salts for collection. Then, the hot high-molecular-weight salts were filtered using a laboratory-scale vacuum filter unit equipped with a 25- $\mu\text{m}$  cloth filter. Meanwhile, the low-molecular-weight salts were collected from the bottom of the tank and filtered while hot. Continuous removal of salts from the top and bottom of the tank and immediate filtration after collection improved salt quality. When the volume of the broth decreased from 1 130 to 190 L, it was quickly transferred to a 227-L tank. Then, removal of salts was repeated for the 227-L tank until all the liquid was completely evaporated.

The filtered carboxylate salts were 45 to 50% moisture; they were dried in a bench-scale oven (120°C, 1.4-kW, Model # 17-Y-11, Precision Scientific Co.). The low-molecular-weight crystallized salts were tightly agglomerated and formed 5-cm chunks. A sand-filled lawn roller was used to crush them and form a powder. The mixed dry salts were stored and passed to the ketonization unit.

### 1.5 Ketonization

Before ketonization, to keep the salts free of excess moisture, the salts were dried in an oven at 104°C for at least 24 hours. The ketone unit had a reaction section and a condensing section. The cylindrical reactor vessel (*Fig. 5*) had a flanged head and a stirrer operated by a motor and seal-less magnetic drive mounted on top. The cylindrical part of the reactor was surrounded by an electric heating jacket (3.8-kW, three-phase, tubular type, Cat # 10-1024-2W, HTS Ampetek Co.). The reactor was constructed from 10-inch-diameter stainless steel schedule-20 pipe with 0.25-in-thick walls. The top flange was 10-in 150-psi class. The bottom plate was 0.5 inch thick. The reactor internal volume was 20 L. Four sintered metal filters (20- $\mu\text{m}$  pore size, 502-cm<sup>2</sup> surface area, custom-made filters, Applied Porous Technology Inc., *Fig. 5*) were installed on the underside of the reactor top flange to prevent solid salt from plugging downstream tubing and blocking the flow of ketone product.

For each batch, 4 kg of mixed carboxylate salts were charged inside the reactor vessel. The reactor head was put in place and tightened. Excess air inside the reactor was removed with a vacuum pump (*Fig. 5*) until the pressure reached 23.4 torr. The vacuum pump was turned off and sweep gas ( $\text{CO}_2$ ) was run through the system at 1 L/min. The reaction was performed at 101 kPa (abs). The condensation system was turned on and the reactor stirring speed was set to 25 rpm. The reactor temperature was set to 420°C. As salts heated to 180-290°C, they went through a plastic state and the stirrer became very hard to turn causing the magnetic drive to slip. Above 290°C, the stirrer again became functional. Routinely, the stirrer was turned off between 180 and 290°C. The reaction was completed after 3 h.

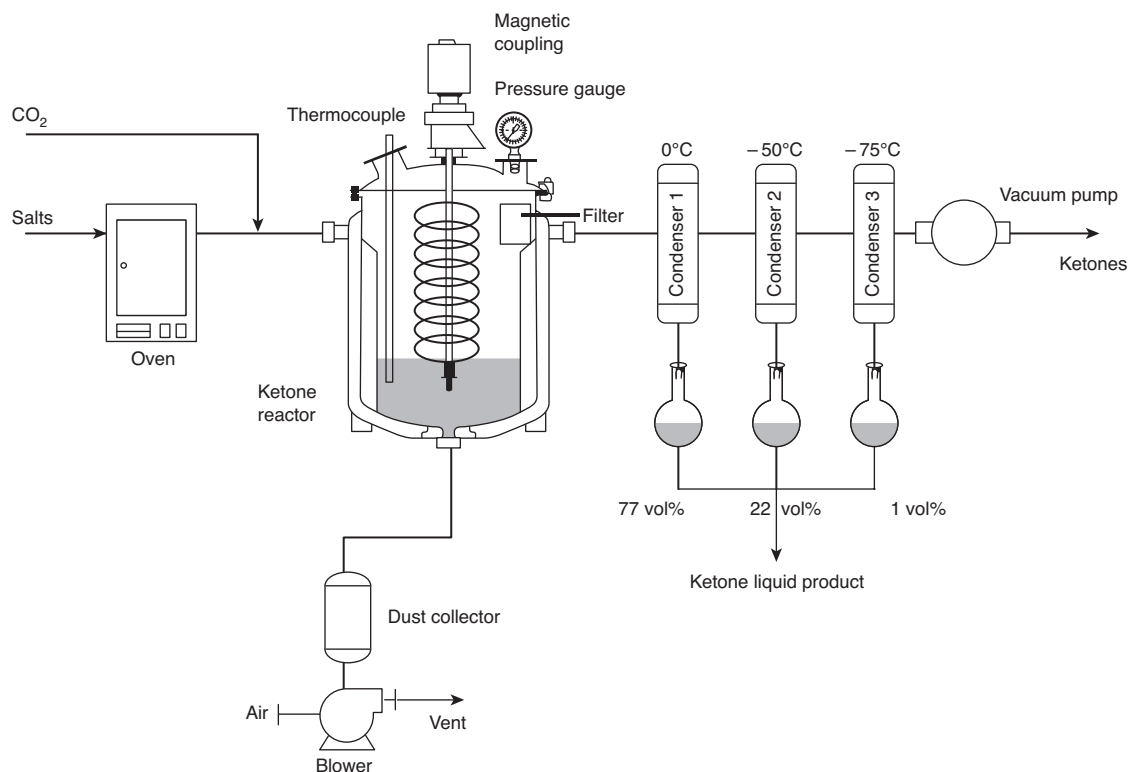


Figure 5

Schematic process flow diagram of the ketone reactor.

The condensing section was a series of three condensers connected to the reactor exit. These condensers progressively cooled the reactor product effluent to 0°C (first condenser), –50°C (second condenser) and –78°C (last condenser). To collect the raw ketones product during each run, a glass flask was mounted below each condenser.

The three condensers were commercial heat exchangers (Model # STS 702-C6-SP, *American Industrial Heat Transfer Inc.*). The 0.57-m-long single-pass heat exchangers had 0.68 m<sup>2</sup> internal surface area. Condenser 1 used a pump to circulate water from an iced-filled beer cooler. After each pass, the water returned to the cooler. The cooler was maintained at nearly 0°C by replenishing ice and draining excess water. Condenser 2 was cooled by a low-temperature recirculation cooler (Model # RC210C0 TLT Recirculating cooler, *SP Industries*), which was equipped with its own internal refrigeration equipment, coolant (*Duratherm XLT-120*) and circulation pump. This cooler could circulate refrigerant from 0 to –80°C. Condenser 3 was cooled by a mixture of dry ice and ethanol. The condensers were made of stainless steel. Most material was collected from Condenser 1.

## 1.6 Distillation

Raw ketones had many impurities (*e.g.*, pyrolysis products) and water, so distillation was necessary to purify the mixture.

If these impurities were not removed, they would adversely affect the downstream hydrogenation process.

The distillation system included a 20-L distillation flask, an electric-resistance heating mantle (1.5-kW, Cat # TM118, *Glas-Col*), a 1-m-long packed column, a condenser connected to a chiller, a receiving flask and a vacuum pump (*Fig. 6*). The flasks and the condenser were constructed of *Pyrex* glass. The column diameter was 10 cm. The column packing was ceramic *Raschig* rings. The coolant liquid from the chiller was a mixture of water and antifreeze 50/50 (vol%).

The raw ketones had a dark brown color. The ketone mixture ranged from acetone (BP = 56°C) to 7-tridecanone (BP = 259°C). To avoid high-temperature distillation, the distillation was divided into two phases: atmospheric and vacuum. For the atmospheric distillation, 15 L of raw ketones were poured into the distillation flask. The first fraction was obtained at 85°C and recovered light ketones (C3–C5). The second fraction was water obtained between 85–90°C. The vapor from this fraction was white and foggy. The condensed water was disposed as a waste material. The third fraction was collected between 90 and 160°C; most of this fraction was C6–C9. The C6–C13 ketones have a low solubility in water (for example 2-hexanone solubility 14 g/L). If some water remained in the third fraction, the collection flask

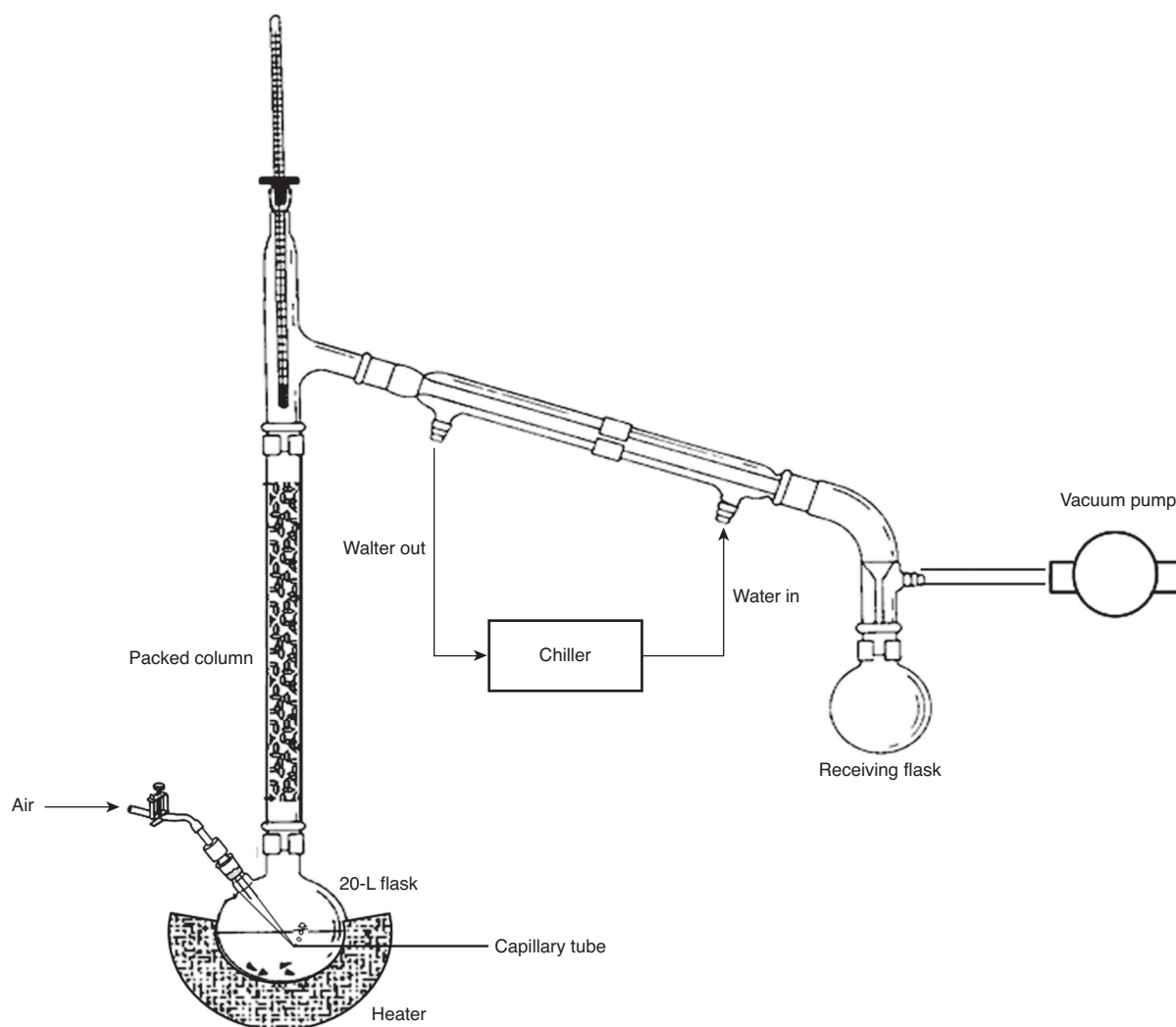


Figure 6  
Schematic process flow diagram of the distillation unit.

would have two layers. Water carries too many impurities and it affects the next catalytic processes, so the water phase was discarded.

For the vacuum distillation fraction, the remaining raw liquid ketones were left in the flask. The vacuum pump was connected to the system and the system generated a pressure of 23.4 torr. Distillate was collected from 60°C to 120°C. To reduce bumping, a capillary tube was placed in the 20-L flask (Fig. 6), which stirred the liquid with gas bubbles. (Note: for convenience air was used as the gas but an inert gas is a better alternative). The distillate obtained above 120°C had a black color, which resulted from oxidation. These oxidized ketones were not collected because they were difficult to hydrogenate. Finally, all the distillate from both the atmospheric and vacuum distillations were mixed and stored with a nitrogen blanket to prevent oxidation.

Table 2 shows the typical volumetric distribution from a distillation. The most abundant cut occurred between 80 and 180°C; 50% of the ketones were obtained between these two temperatures.

TABLE 2  
Ketone distillation distribution

	Compounds	Amount (vol%)
Atmospheric distillation 80°C	C3–C5	15
Atmospheric distillation 90–180°C	C5–C10	49.9
Vacuum distillation 120°C	C10–C13	27.8
Water	H <sub>2</sub> O	7.3
Total		100



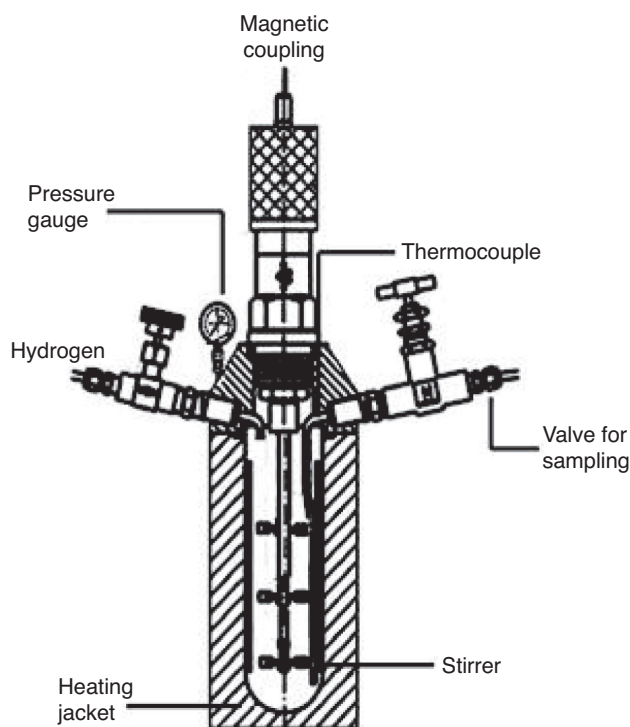


Figure 7  
Schematic diagram of the batch hydrogenation reactor.

## 1.7 Hydrogenation

Hydrogenation was performed in a 7.5-L stainless steel batch reactor (230-V, 2.3-kW Parr Model # 4522M Press React APP26 Cart-MA) (Fig. 7). The catalyst was Raney nickel (Cat # 221678, Sigma Aldrich). The catalyst was in a slurry form with water (50% Raney nickel). The hydrogen was industrial quality from Praxair Inc. The batch reactor was equipped with a magnetic drive connected to the stirrer (0-1000 rpm) for mixing (Fig. 7). The temperature inside the reactor was monitored *via* a thermocouple and regulated *via* a controller connected to a heating jacket.

First, 5 L of distilled ketones and 100 mL of Raney nickel catalyst were charged to the reactor. The reactor head was put in place and tightened. Excess air inside the reactor was purged with hydrogen. Hydrogen was added until the reactor pressure reached 69 bar (abs). The stirrer rotated at 750 rpm. The heating jackets increased the reaction temperature to 155°C. During heating, fresh hydrogen was added to maintain the reactor pressure at 69 bar (abs). After the temperature stabilized to 155°C, fresh hydrogen was added until the reactor pressure was 86 bar (abs). The stabilization time was 1 h and the reaction was completed after 24 h. All the products

were collected and analyzed in a gas chromatograph-mass spectrograph (GC-MS, HP Model G1800C). The alcohol product was collected and centrifuged to separate the catalyst from the liquid. The used catalyst was placed back into the reactor and used for the next batch. Finally, 100 mL of fresh catalyst was added and the procedure was repeated.

## 1.8 Oligomerization

The mixture of alcohols ranged from C3 to C13 and was the feed for all the oligomerization experiments. Oligomerization was performed in a reactor unit consisting of two packed-bed Plug-Flow Reactors (PFR), a pre-heater, an HPLC pump, two condensers, Back Pressure Regulator (BPR), Control Valve (CV), Relief Valve (RV) and gas lines for nitrogen and air (Fig. 8). The reactor and the pipes were constructed of 316-type stainless steel.

The pump injected liquid into the preheater (410°C) to vaporize it. After the liquid became a vapor, it went through PFR 1, where it contacted the HZSM-5 catalyst, which dehydrated the alcohols and produced water. The reaction products went through Condenser 1, which was ice-cooled ( $T = 0^{\circ}\text{C}$ ) to separate the liquid and gas. The liquid had two phases: hydrocarbon and water on the bottom. Because the gases were mainly C3 and C4, they were further oligomerized in PFR 2. About every hour, the liquid from Condenser 1 was collected by opening Valve 2 (V2) for approximately 3 min until all the liquid was collected. A (BPR) with a set point of 377 kPa (abs) was connected to the end of Condenser 2.

The catalyst was HZSM-5 purchased from Zeolyst International in Malvern, PA (product # CBV 28014,  $\text{SiO}_2/\text{Al}_2\text{O}_3 = 280$ , surface area = 400  $\text{m}^2/\text{g}$ , 20% alumina binder). The manufacturer supplied cylindrical extruded pellets (diameter = 1.6 mm, length = 3.5 mm), which were packed near the middle section of the reactor. The top and bottom sections of the reactor were filled with  $\alpha\text{-Al}_2\text{O}_3$  as an inert packing before and after the catalytic bed. As received, the catalyst had a total acidity (determined by  $\text{NH}_3\text{-TPD}$ ) of 0.79 mmol/g in which weak and strong acids were 0.42 and 0.37 mmol/g, respectively [9]. To obtain an acid structure, the catalyst was activated with a  $\text{N}_2$  stream at 550°C for 1 h, which drove off the ammonia [10]. Chang and Silvestri [11] published the first experimental results showing the effectiveness of catalyst HZSM-5 for converting methanol to gasoline. The reaction products of HZSM-5 ranged from C1 to C11 hydrocarbons and gasoline ranges from C5 to C11. Unlike other zeolites, HZSM-5 does not deactivate greatly over time [12]; thus, HZSM-5 was chosen as catalyst in the oligomerization step. More details are found in the literature [13].

PFR 1 contained 50 g of catalyst HZSM-5 (280) whereas PFR 2 contains 60 g of the same catalyst. The alcohol feed rate was characterized by the Weight Hourly Space Velocity (WHSV).

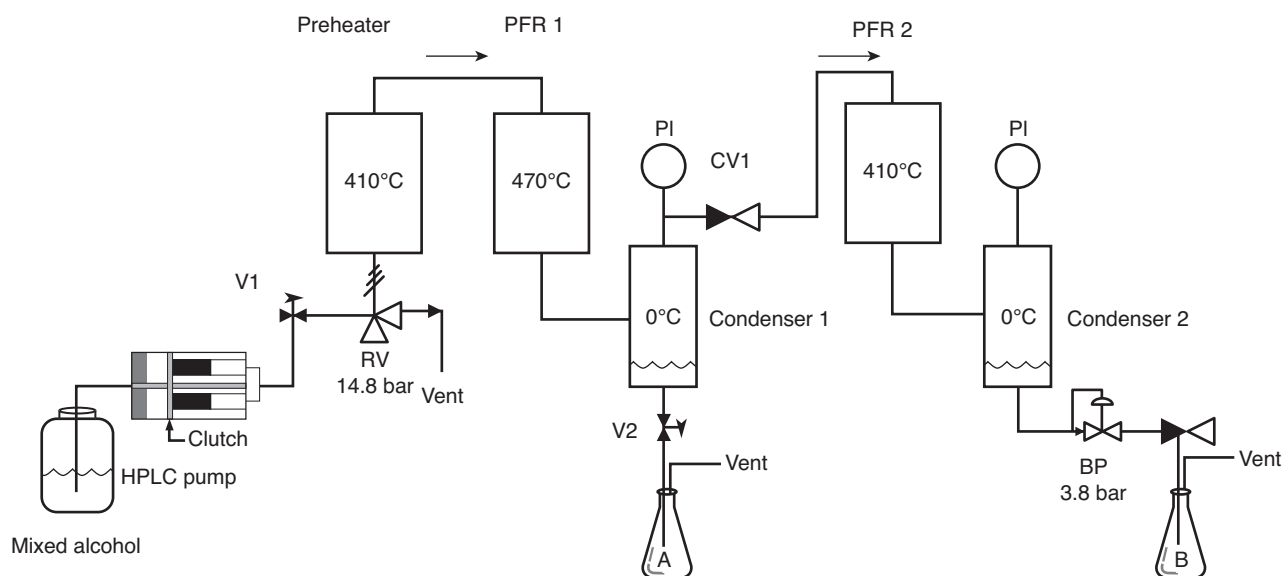


Figure 8

Schematic diagram of the oligomerization apparatus. (Note: pressures are absolute).

The WHSV is defined as the weight of feed per hour per unit weight of catalyst loaded in the reactor:

$$\text{WHSV} = \frac{\dot{m}_{\text{feed}}}{m_{\text{catalyst}}} \quad \text{where:}$$

$$\dot{m}_{\text{feedstock-feed}} = \text{mass flow rate to the reactor (g/h)}$$

$$m_{\text{catalyst}} = \text{mass of catalyst (g)}$$

For example, if the feed rate is 10 g per hour to the reactor and 10 g of catalyst loaded in the reactor, the WHSV is  $1.0 \text{ h}^{-1}$ .

During preliminary experiments performed in a smaller reactor (diameter = 10 mm, length = 357 mm), WHSV between  $0.5$  and  $10 \text{ h}^{-1}$  could dehydrate the mixed alcohol; thus, PFR 1 could process up to 600 mL/h of mixed alcohol. To be conservative, about 300 mL/h was pumped into the system. The hydrocarbon liquid from PFR 1 was called Product A whereas the hydrocarbon liquid from PFR 2 was called Product B.

GC-MS analysis of the liquid phase typically determined that the liquid samples have over 100 compounds. The compounds were described by carbon number and types of products (*i.e.*, paraffins, oxygenated compounds, olefins, naphthenes, naphthenes olefinics and aromatics). The carbon number ranges from C4 to C14.

## 1.9 Olefin Hydrogenation

Hydrocarbon Products A and B were mixed and hydrogenated. Hydrogenation was performed in the same batch reactor used

for mixed alcohols. The catalyst was Raney nickel in a slurry form with water (50% Raney nickel). The hydrogenation followed the same steps as the ketone hydrogenation. Except for pressure and reaction time, all other conditions were the same. The reactor pressure was set at 21.7 bar (abs) and the reaction time was only 3 h. All the products were collected and analyzed in a gas chromatograph-mass spectrograph (GC-MS, HP Model G1800C). The saturated hydrocarbon product was collected and centrifuged to separate the catalyst from the liquid.

## 2 RESULTS AND DISCUSSION

### 2.1 Fermentation

Figure 9 shows an example of the initial fermentation, which operated in batch mode. After 30 days, the total acid concentration reached  $27.61 \pm 1.34 \text{ g/L}$ . During fed-batch operation, every 7 to 10 days, the total acid concentration reached  $\sim 15 \text{ g/L}$ . Figure 10 shows a typical concentration distribution of carboxylic acids in RFB.

### 2.2 Descumming

Figure 11 shows the carboxylic acid distribution for RFB, descummed RFB and descummed-and-centrifuged RFB. The compositions are nearly identical in each stream, so the descumming process had no effect on the acid distribution.

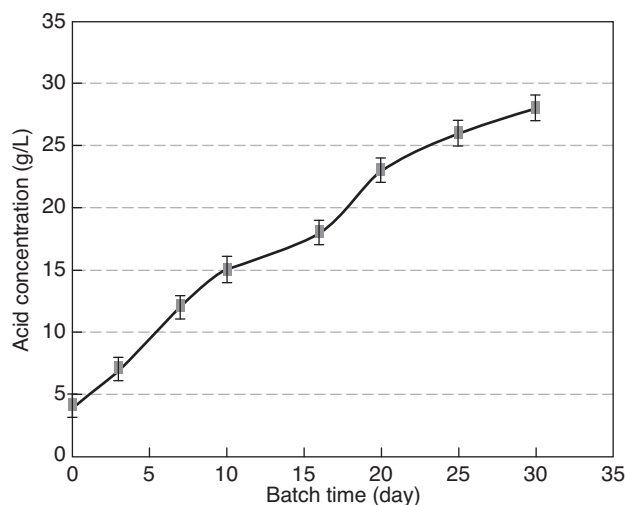


Figure 9

Total mixed carboxylic acids concentration in batch fermentation. (Error bars are  $\pm 2\sigma$ ).

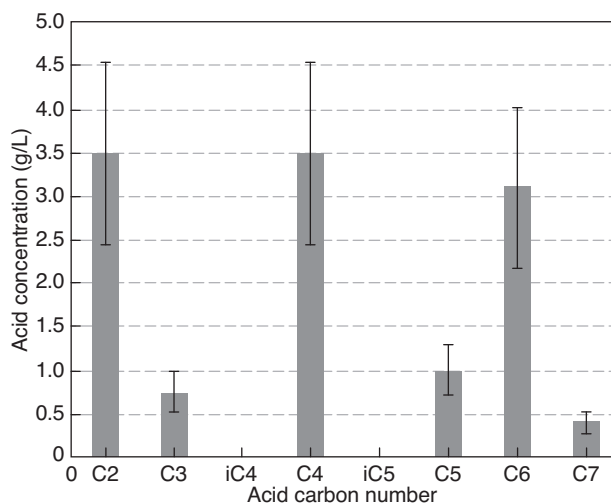


Figure 10

Distribution of mixed carboxylic acids in raw broth harvested from fermentor operated in fed-batch mode. (Error bars are  $\pm 2\sigma$ ).

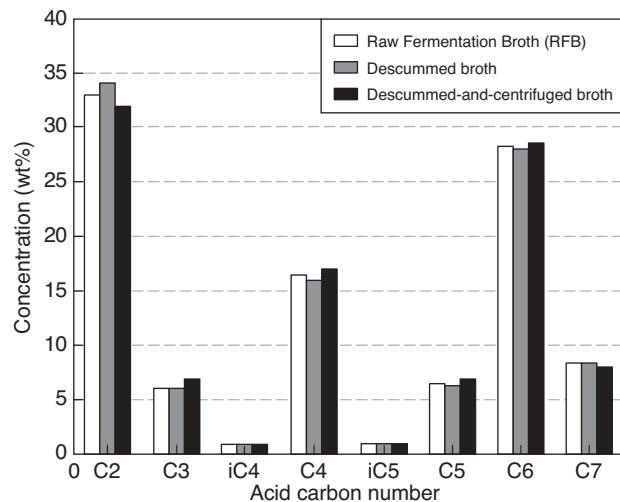


Figure 11

Effect of descumming and centrifuging on the distribution of carboxylic acids.

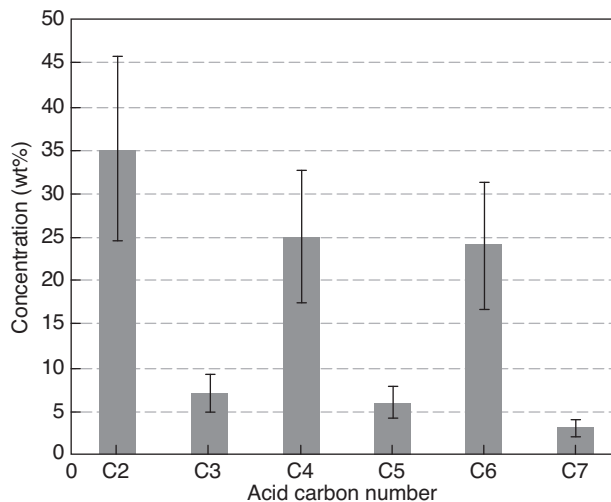


Figure 12

Distribution of carboxylic acids in the descummed dry salts. (Error bars are  $\pm 2\sigma$ ).

### 2.3 Dewatering and Crystallization

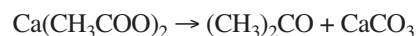
Figure 12 shows the typical distribution of acids in the dry mixed carboxylate salts used in the ketonization process. In mixed acid salts, the average weight ratio of low-molecular-weight acids mostly (C2–C3 acids) to high-molecular-weight acids (C4–C7) was 1:1.

### 2.4 Ketonization

Table 3 shows the average acid distribution in the salts sent to the ketonization reactor. The distributions were taken from

the average mass concentration presented in Figure 12 and were transformed to mole fraction using the molecular weight of the salts.

The carboxylate salts produced not only ketones but also calcium carbonate ( $\text{CaCO}_3$ ). For example, the ketonization of calcium acetate follows:



In the salts, one calcium is ionically bonded with two carboxylates, which can have the same or different carbon numbers ranging from C2 to C7. During the ketonization reaction,

TABLE 3  
Average acid distribution of the descummed dry salts

Acid	Concentration (wt%)	Concentration (mol%)	Salt MW	Theoretical CaCO <sub>3</sub> (wt%)
C2	35	46.6	158	22.2
C3	7	7.6	186	3.8
C4	25	22.7	214	11.7
C5	6	4.7	242	2.5
C6	24	16.5	270	8.9
C7	3	1.8	298	1.0
Total	100	100.0		50.0

TABLE 4  
Experimental and theoretical ketone product distribution

Acid pair	Probability (mol%)	Ketone product	Theoretical concentration (wt%)	Experimental concentration (wt%)
C2 × C2	21.75	2-propanone	12.9	7.5
C2 × C3	7.05	2-butanone	5.2	3.3
C2 × C4	21.18	2-pentanone	18.6	9.5
C2 × C5	4.39	2-hexanone	4.5	5.2
C2 × C6	15.43	2-heptanone	18.0	21.4
C2 × C7	1.72	2-octanone	2.3	4.6
C3 × C3	0.57	3-pentanone	0.5	
C3 × C4	3.44	3-hexanone	3.5	2.4
C3 × C5	0.71	3-heptanone	0.8	
C3 × C6	2.50	3-octanone	3.3	3.6
C3 × C7	0.28	3-nonanone	0.4	4.3
C4 × C4	5.16	4-heptanone	6.0	3.0
C4 × C5	2.14	4-octanone	2.8	2.0
C4 × C6	7.51	4-nonanone	10.9	12.4
C4 × C7	0.84	4-decanone	1.3	
C5 × C5	0.22	5-nonanone	0.3	
C5 × C6	1.56	5-decanone	2.5	7.0
C5 × C7	0.17	5-undecanone	0.3	
C6 × C6	2.74	6-undecanone	4.8	11.1
C6 × C7	0.61	6-dodecanone	1.1	2.3
C7 × C7	0.03	7-tridecanone	0.1	0.4
Total	100.00		100.0	100.0

the salt composition determines the ketone composition. Assuming random pairing, Table 4 shows all the acid-pair combinations and the theoretical ketone product. Because the molar concentration of the salt mixture was known, the probable

molar concentration for each ketone product was found (Tab. 4). For example, the acetate molar concentration in the salts was 46.6 mol% (Tab. 3); so the molar probability of obtaining acetone was 21.7 mol% ( $46.6 \times 46.6/100$ ). Finally, the mass concentration for the ketone mixture was calculated and compared to the experimental values. Landoll [5] provides an alternative model (Gibbs free energy minimization) to predict ketone profiles better than random pairing. The model considers both the thermodynamic and kinetic aspects of the thermal decomposition, as well as the production of by-products.

## 2.5 Hydrogenation

Mixed-ketone hydrogenation was performed with the following conditions:  $T = 155^\circ\text{C}$ ,  $P = 86$  bar (abs),  $t = 24$  h and 100 mL Raney nickel catalyst per 5 L ketones. Figure 13 shows the carbon distribution for the alcohols.

## 2.6 Oligomerization

Figure 14 shows the mass balance with 100 g of mixed alcohol as the basis. Table 5 shows the composition of Product A. The most abundant products are linear olefins (70%) and branched olefins (12%). It is noteworthy that dehydration occurred on PFR 1 because olefins are the most abundant in Product A. The average carbon number is 7.84. Table 6 shows the product distribution for Product B. The most abundant products are aromatics (72%) and branched olefins (16%). These results illustrate that oligomerization is predominant on PFR 2. The average carbon number is 8.57, which is slightly higher than Product A.

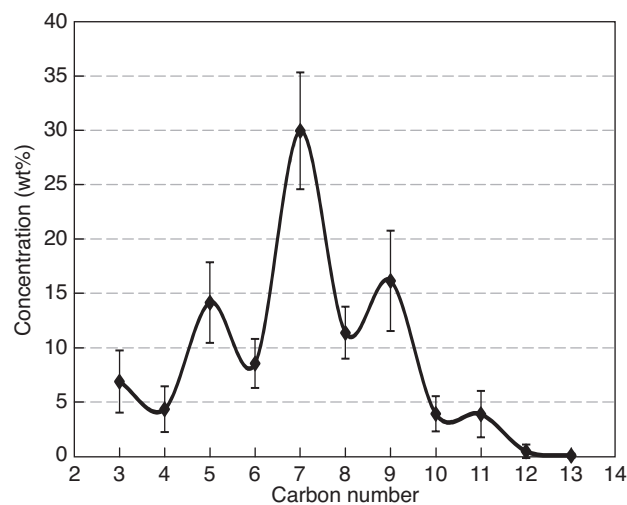


Figure 13

Distribution of alcohols obtained from the hydrogenation. (Error bars are  $\pm 1\sigma$ ).

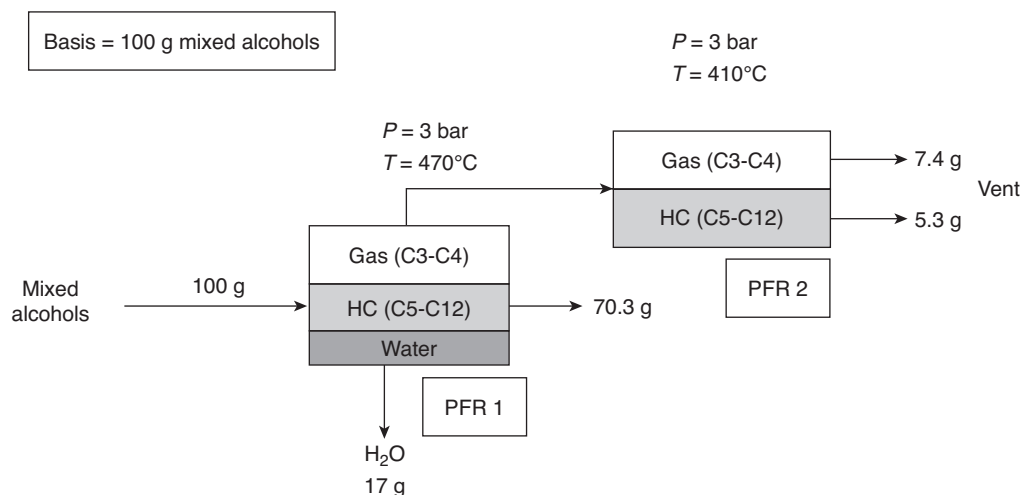


Figure 14

Mass balance for mixed alcohol oligomerization reaction before optimization.

TABLE 5

Product A liquid carbon distribution of mixed alcohol reaction using HZSM-5 (280), WHSV =  $6 \text{ h}^{-1}$ ,  $P = 3 \text{ bar}$  (abs)

C#	Paraffins	Linear olefins	Isoparaffins	Naphthenes	Branched olefins	Aromatics	Total
5	0	4.3	0	0	0	0	4.3
6	0	0	0	0	9.7	0	9.7
7	0	37.2	1.7	0	0	0.5	40.4
8	0	14.3	0	0	0.3	1.4	16.0
9	0.3	8.6	0	0	2.8	1.2	14.4
10	0	1.4	0.9	0.4	0	2.3	5.9
11	1.8	3.0	0	1.8	0	0.7	7.3
12	0.7	0.5	0	0	0	0.9	2.1
Total	2.8	69.2	2.6	2.3	12.8	7.0	100.0

TABLE 6

Product B liquid carbon distribution of mixed-alcohol reaction using HZSM-5 (280), WHSV =  $1.33 \text{ h}^{-1}$ ,  $P = 3 \text{ bar}$  (abs)

C#	Paraffins	Linear olefins	Isoparaffins	Naphthenes	Branched olefins	Aromatics	Total
5	0	0	0	0.0	5.0	0.0	5.0
6	0	0	0	0.6	3.2	0.0	3.8
7	0	0	0	1.5	0.5	6.2	8.2
8	0	0	0	8.0	0.7	29.2	37.9
9	0	0	0	1.1	5.6	15.3	22.0
10	0	0	0	0.4	0.0	7.8	8.2
11	0	0	0	0.5	1.1	7.9	9.6
12	0	0	0	0.0	0.0	4.1	4.1
13	0	0	0	0.0	0.0	1.0	1.0
Total	0	0	0	12.2	16.2	71.5	100.0

## 2.7 Olefin Hydrogenation

Olefin conversion was 100%. After hydrogenation, branched olefins became isoparaffins and linear olefins became paraffins. Branched and linear olefins were saturated. Aromatics were not hydrogenated because the conditions were mild.

## CONCLUSIONS

From waste office paper and chicken manure, the pilot-scale experiments produced synthetic gasoline that can be blended into the commercial gasoline pool. Preliminary economic evaluations indicate that a commercial-scale process can sell gasoline for about \$2.56/gal (\$0.68/L) in the base-case scenario, with a range from \$1.25/gal (\$0.33/L) to \$3.75/gal (\$0.99/L), depending upon assumptions [1].

## ACKNOWLEDGMENTS

Appreciation is given to Dr. John Dunkleman, Austin Bond and Swades K. Chaudhurib for their help with this project. Appreciation is also given to Dr. Mannan for use of his GC-MS.

## REFERENCES

- 1 Pham V., Holtzapple M., El-Halwagi M. (2010) Techno-economic analysis of biomass to fuel conversion via the MixAlco process, *J. Ind. Microbiol. Biotechnol.* **37**, 1157-1168.
- 2 Holtzapple M., Davison R., Ross M., Aldrett-Lee S., Nagwani M., Lee C.-M., Lee C., Adelson S., Kaar W., Gaskin D., Shirage H., Chang N.-S., Chang V., Loescher M. (1999) Biomass conversion to mixed alcohol fuels using the MixAlco process, *Appl. Biochem. Biotechnol.* **79**, 1, 609-631.
- 3 Holtzapple M., Granda C. (2009) Carboxylate platform: The MixAlco process Part 1: Comparison of three biomass conversion platforms, *Appl. Biochem. Biotechnol.* **156**, 1-3, 95-536.
- 4 Granda C., Holtzapple M., Luce G., Searcy K., Mamrosh D. (2009) Carboxylate platform: The MixAlco process. Part 2: Process economics, *Appl. Biochem. Biotechnol.* **156**, 1-3, 107-554.
- 5 Landoll M., Holtzapple M. (2011) Thermal decomposition of mixed calcium carboxylate salts: Effects of lime on ketone yield, *Biomass Bioenergy* **35**, 8, 3592-3603.
- 6 Chang N., Aldrett S., Holtzapple M., Davison R. (2000). Kinetic studies of ketone hydrogenation over Raney nickel catalyst, *Chem. Eng. Sci.* **55**, 23, 5721-5732.
- 7 Zhu L., O'Dwyer J.P., Granda C., Holtzapple M. (2008) Structural features affecting biomass enzymatic digestibility, *Bioresour. Technol.* **99**, 9, 3817-3828.
- 8 Chang V., Holtzapple M. (2000) Fundamental Factors Affecting Biomass Enzymatic Reactivity, *Appl. Biochem. Biotechnol.* **84-86**, 5-37.
- 9 Gaigneaux E. (ed.) (2010) Scientific bases for the preparation of heterogeneous catalysts, *10th International Symposium on the Scientific Bases for the Preparation of Heterogeneous Catalysts*, Louvain-la-Neuve, Belgium, Amsterdam, 10-15 July.
- 10 Yoon J., Chang J., Lee H., Kim T., Jung S. (2007) Trimerization of isobutene over a zeolite beta catalyst, *J. Catal.* **245**, 1, 253-256.
- 11 Chang C., Silvestri A. (1977) Conversion of methanol and other O-compounds to hydrocarbons over zeolite catalysts, *J. Catal.* **47**, 249-259.
- 12 Chang C. (1983) *Hydrocarbon from Methanol*, Marcel Dekker Inc., New York.
- 13 Taco-Vasquez S. (2012) *Transformation of Acetone and Isopropanol to Hydrocarbons*, Lap Lambert Academic Publishing, Berlin.

Final manuscript received in September 2012  
Published online in April 2013